A dynamic organic soil biogeochemical model for simulating the effects of wildfire on soil environmental conditions and carbon dynamics of black spruce forests

Shuhua Yi,[1] A. David McGuire,[2] Eric Kasischke,[3] Jennifer Harden,[4] Kristen Manies,[4] Michelle Mack,[5] and Merritt Turetsky[6]

Received 25 January 2010; revised 7 July 2010; accepted 2 August 2010; published 4 November 2010.

[1] Ecosystem models have not comprehensively considered how interactions among fire disturbance, soil environmental conditions, and biogeochemical processes affect ecosystem dynamics in boreal forest ecosystems. In this study, we implemented a dynamic organic soil structure in the Terrestrial Ecosystem Model (DOS-TEM) to investigate the effects of fire on soil temperature, moisture, and ecosystem carbon dynamics. DOS-TEM consists of environmental, ecological, disturbance effects, and dynamic organic soil modules. Changes in organic layer thickness are computed from calculated changes in carbon pools following fire and during stand succession. DOS-TEM was parameterized based on studies reported in the literature and evaluated independently at sites in interior Alaska. This evaluation reveals that (1) DOS-TEM is capable of accurately simulating the thickness and carbon content of organic soils; and (2) without the dynamic linkage between soil organic thickness and carbon content, the model overestimates soil carbon in deep mineral soil horizons of dry black spruce ecosystems of interior Alaska. Sensitivity tests were performed to investigate issues related to spatial heterogeneity of carbon dynamics including soil drainage and fire frequency. Results show that both soil drainage and fire frequency are important in the carbon dynamics simulated by DOS-TEM, and should be considered in spatial applications of the model.

Citation: Yi, S., A. D. McGuire, E. Kasischke, J. Harden, K. Manies, M. Mack, and M. Turetsky (2010), A dynamic organic soil biogeochemical model for simulating the effects of wildfire on soil environmental conditions and carbon dynamics of black spruce forests, *J. Geophys. Res.*, *115*, G04015, doi:10.1029/2010JG001302.

1. Introduction

[2] Wildfire is an important disturbance in boreal forest ecosystems of North America [*Kasischke et al.*, 2006] and a growing number of studies indicate that wildfire plays an important role in the carbon (C) dynamics of northern high-latitude ecosystems [*Zimov et al.*, 1999; *Harden et al.*, 2000; *Bond-Lamberty et al.*, 2007; *Balshi et al.*, 2007, 2009a]. The frequency of large fires has increased dramatically in the North American boreal forest region over the past four decades [*Gillett et al.*, 2004; *Kasischke and Turetsky*, 2006], and it is projected to increase further throughout this century in response to projected climate warming [*Flannigan et al.*, 2005; *Balshi et al.*, 2009b]. Because northern high-latitude regions contain large amounts of soil C [*Schuur et al.*, 2008; *Tarnocai et al.*, 2009], it is important to properly represent how interactions among fire, soil environmental conditions and biogeochemical processes influence soil C storage in the region to understand the potential for these interactions to affect the climate system [*McGuire et al.*, 2009].

[3] Wildfire affects the C balance of boreal ecosystems directly through combustion of vegetation and near-surface soil organic horizons [*Kasischke et al.*, 2005], and indirectly through the changes of surface energy balance [*Liu et al.*, 2005], soil thermal and hydrological regimes [*MacKay*, 1995; *Burn*, 1998; *O'Neill et al.*, 2002; *Kasischke and Johnstone*, 2005; *Liljedahl et al.*, 2007], and vegetation succession [*Johnstone and Kasischke*, 2005; *Johnstone and Chapin*, 2006]. At the regional scale, the direct effects of fire have received much attention [*Thonicke et al.*, 2001; *Arora and Boer*, 2005; *Balshi et al.*, 2007], but the evaluation of the indirect effects of fire has been limited because the appropriate tools have not yet been fully developed for application at the regional scale. With an increase in understanding the importance of organic soil on soil thermal and hydrological regimes, regional land surface and terrestrial

[1] State Key Laboratory of Cryosphere Sciences, Cold and Arid Regions Environmental and Engineering Research Institute, Lanzhou, China.
[2] Alaska Cooperative Fish and Wildlife Research Unit, U.S. Geological Survey, University of Alaska Fairbanks, Fairbanks, Alaska, USA.
[3] Department of Geography, University of Maryland, College Park, Maryland, USA.
[4] U.S. Geological Survey, Menlo Park, California, USA.
[5] Department of Botany, University of Florida, Gainesville, Florida, USA.
[6] Department of Integrative Biology, University of Guelph, Guelph, Ontario, Canada.

0148-0227/10/2010JG001302

ecosystem models have begun to implement organic matter horizons into their representations of the soil profile [*Zhuang et al.*, 2001; *Zhang et al.*, 2003; *Yi et al.*, 2006; *Lawrence and Slater*, 2008]. Some site-specific modeling studies have represented changes in the thickness of organic horizons after fire based on the balance between litter input and soil C decomposition [*Carrasco et al.*, 2006; *Fan et al.*, 2008; also see *Frolking et al.*, 2001], but these studies did not consider how those changes affect soil temperature and moisture dynamics. To our knowledge, none of the modeling efforts to date have dynamically represented how changes in the thickness of organic horizons caused by disturbance and subsequent postfire changes in organic layer thickness influence interactions among soil thermal, hydrological, and biogeochemical dynamics. In this study we describe the development and evaluation of a dynamic organic soil version of the Terrestrial Ecosystem Model (TEM) that is capable of representing the influence of changes in organic soil thickness on the dynamics of northern high-latitude terrestrial ecosystems. This new version of TEM explicitly represents how dynamic changes in the thickness of organic horizons influence soil thermal, hydrological and biogeochemical dynamics to affect C exchange with the atmosphere.

[4] Black spruce (*Picea mariana* (Mill.)) forests are one of the most common ecosystem types in the North American boreal forest, and have surface organic horizons that range in thickness from 10 to > 40 cm [*Viereck and Johnston*, 1990]. Because of their deep organic horizons, they play an important role in the C dynamics of boreal North America [*Clein et al.*, 2002]. We therefore evaluated the model described in this study for its ability to simulate the structure of organic soils in black spruce forest ecosystems at study sites located near Delta Junction in interior Alaska. As part of this evaluation we conducted a sensitivity analysis to understand the importance of considering a dynamic versus static soil organic layer on soil thermal, hydrological, and C dynamics over a 900 year period of a repeatedly burned intermediately drained black spruce forest stand. We also conducted two site-specific sensitivity analyses focused on issues related to spatial heterogeneity across the range of black spruce forests in North America that have the potential to substantially influence the structure and function of soil organic horizons in these ecosystems: soil water drainage and fire frequency [*Harden et al.*, 2000].

2. Methods

2.1. Model Development

[5] The Terrestrial Ecosystem Model (TEM) is a process-based ecosystem model designed to simulate the C and nitrogen (N) pools of vegetation and soil, and the C and N fluxes among vegetation, soil, and the atmosphere. The TEM has evolved substantially over the last two decades from an equilibrium biogeochemical model applied at continental and global scales [*Raich et al.*, 1991; *McGuire et al.*, 1992; *Melillo et al.*, 1993], and now represents how biogeochemical dynamics of northern high-latitude ecosystems are affected at seasonal to century scales by processes like soil thermal dynamics [*Zhuang et al.*, 2001, 2002, 2003], snow cover [*Euskirchen et al.*, 2006, 2007], and fire [*Balshi et al.*, 2007, 2009a]. While previous model development efforts have improved the soil thermal and hydrological processes in TEM for application in high-latitude regions [*Zhuang et al.*, 2001, 2002; *Euskirchen et al.*, 2006], fire disturbance implemented in these model versions reduced the amount of soil C without affecting organic soil thickness and associated changes in the thermal and hydrological properties of soil [e.g., *Balshi et al.*, 2007, 2009a]. To prepare TEM for dynamically simulating soil organic C dynamics, *Yi et al.* [2009a] modified the model version of TEM used by *Balshi et al.* [2007, 2009a] by coupling soil thermal and hydrological processes of TEM so that the model is capable of simulating soil environmental changes in the context of changing soil organic thickness. Here we describe the further modifications of TEM that were required for the model to compute changes in organic layer thickness from calculated changes in carbon pools following fire and during stand succession.

[6] There are four components in dynamic organic soil version TEM (hereafter DOS-TEM): the environmental module (EnvM), the ecological module (EcoM), the fire effects module (FEM), and the dynamic organic soil module (DOSM) (Figure 1). The purpose of the EnvM is to provide the EcoM with information on the atmospheric and soil environment and to provide the FEM with information on the soil environment. Specifically, the EnvM calculates the dynamics of biophysical processes driven by data on climate, topography, mineral soil texture, leaf area index (from the EcoM), and soil structure (from the DOSM) (Figure 1). Soil temperature and moisture conditions are calculated for multiple layers within various soil horizons including moss, fibric organic, amorphous organic, and mineral horizons. A detailed description of EnvM is provided in the appendix of *Yi et al.* [2009a], and an overview of EnvM can be found in Appendix A of this paper.

[7] The EcoM uses the information on atmospheric chemistry, the atmospheric and soil environmental conditions calculated by the EnvM, the soil structure (from the DOSM), and the fate of soil and vegetation C and N pools (from the FEM) to simulate vegetation and soil C and N pools of the ecosystem (Figure 1). Information on soil carbon changes is provided to the DOSM yearly so that it can alter the thicknesses of soil organic horizons. The FEM has been designed to calculate the fate of vegetation C and N pools driven by information on fire occurrence, topography, the soil environment (from the EnvM), and the soil structure (from the DOSM) (Figure 1). Below we provide expanded overviews of the EcoM, FEM, and DOSM; detailed descriptions of these modules can be found in Appendices B–D of this paper.

[8] The EcoM simulates the C and N pools of vegetation and soil, and the C and N fluxes among vegetation, soil and atmosphere (Figure 2). In contrast to previous versions of TEM, DOS-TEM simulates the dynamics of three different soil C horizons (the fibrous, amorphous, and mineral soil horizons). Because the decomposition parameters used in the model are defined separately for each horizon, this version of TEM is capable of representing multiple soil of different quality that are stratified vertically. The C from vegetative litterfall is divided into aboveground litterfall and belowground litterfall. Aboveground litterfall is assigned only to the first layer of the fibrous horizon, while belowground litterfall is assigned to different layers of the three

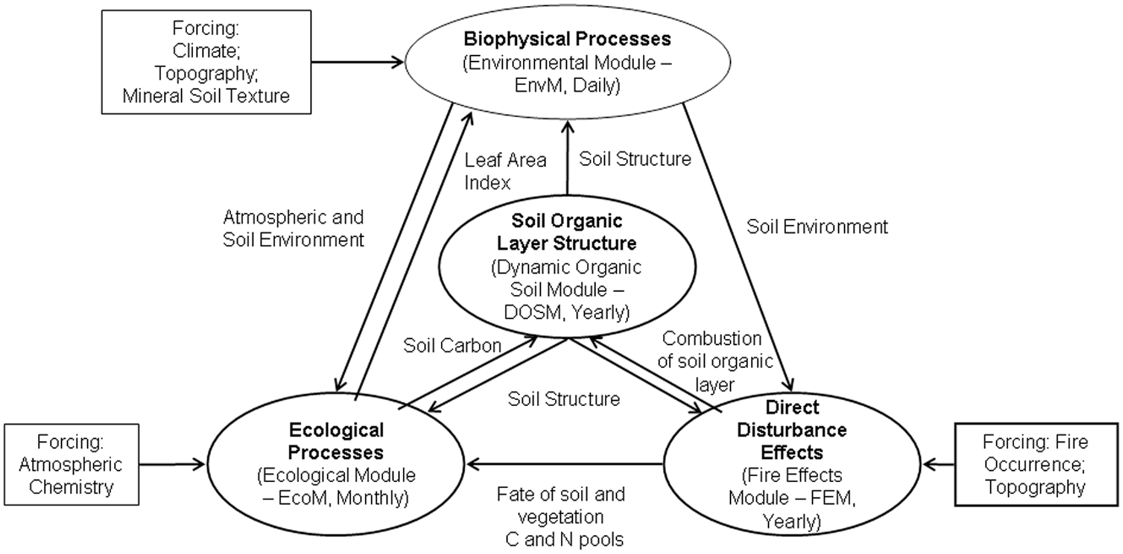

Figure 1. Interactions among modules of the dynamic organic soil version of the Terrestrial Ecosystem Model (DOS-TEM). Modules include the daily environmental module (EnvM), the monthly ecological module (EcoM), the annual fire effects module (FEM), and the dynamic organic soil module (DOSM).

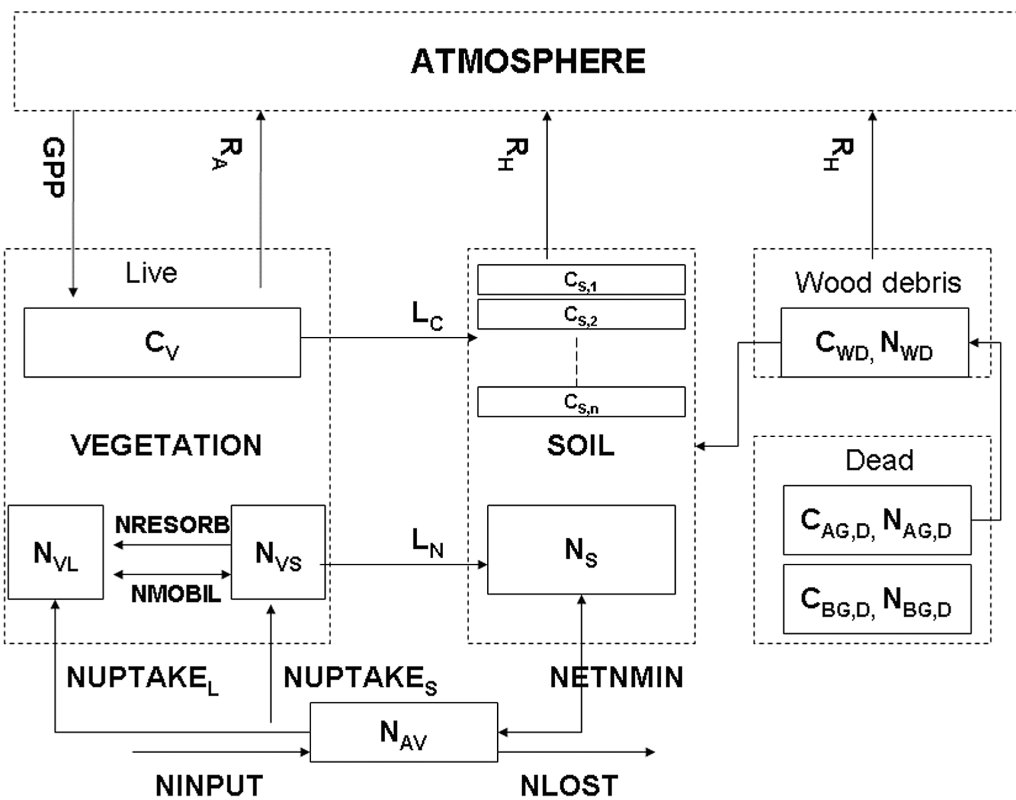

Figure 2. The carbon and nitrogen pools and fluxes of the ecological module in the dynamic organic soil version of the Terrestrial Ecosystem Model (DOS-TEM). R_A, autotrophic respiration; GPP, gross primary production; R_H, heterotrophic respiration; C_V, vegetation carbon; N_{VL}, labile vegetation nitrogen; N_{VS}, structural vegetation nitrogen; L_C, litterfall carbon; L_N, litterfall nitrogen; $C_{S,I}$, soil carbon of layer i; N_S, soil organic nitrogen; N_{AV}, available soil inorganic nitrogen; WD, woody debris; AG, aboveground; BG, belowground; D, dead; $NUPTAKE_L$, N uptake into the labile N pool of the vegetation; $NUPTAKE_S$, N uptake into the structural N pool of the vegetation; NETNMIN, net N mineralization of soil organic N; NINPUT, N inputs from outside the ecosystem; and NLOST, N losses from the ecosystem.

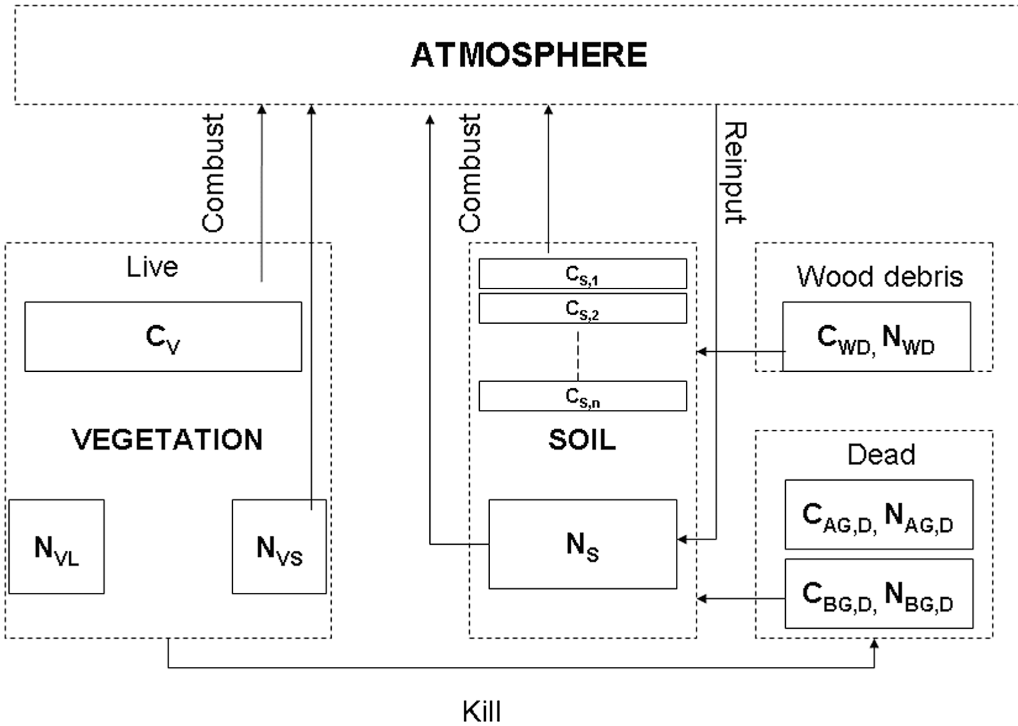

Figure 3. The fate of carbon and nitrogen at the time of fire as defined by the fire effects module of the dynamic organic soil version of Terrestrial Ecosystem Model (DOS-TEM). C_V, vegetation carbon; N_{VL}, labile vegetation nitrogen; N_{VS}, structural vegetation nitrogen; $C_{S,I}$, soil carbon of layer i; N_S, soil organic nitrogen; WD, woody debris; AG, aboveground; BG, belowground; D, dead.

horizons based on the fractional distribution of fine roots with depth. The dynamics of coarse woody debris, an important C pool associated with fire disturbance in the boreal forest [*Manies et al.*, 2005], is also considered in DOS-TEM. EcoM is run at monthly time step.

[9] The FEM simulates how fire affects C and N pools of vegetation and soil, including combustion emissions to the atmosphere, the fate of uncombusted C and N, and the flux of N from the atmosphere to the soil via biological N fixation in the years following a fire (Figure 3). The amount of soil C combusted is determined by comparing the distribution of soil C with depth to the depth of burn estimated by the FEM. At the time of fire, aboveground vegetation C and N are divided into three parts: live aboveground vegetation C (1% of prefire aboveground vegetation C), uncombusted dead aboveground C (76%), and combusted aboveground C (23%). The belowground vegetation C is divided into three parts: belowground live root C (1% of prefire root C), uncombusted dead root C, and combusted root C. The amounts of uncombusted and combusted root C are determined by comparing the prefire root C with the depth of burning into the organic soil horizons. N generally follows the fate of C based on C:N ratios of vegetation and soil with the exception that some volatilized N is retained by the ecosystem [*Harden et al.*, 2004]. The net amount of N lost from the ecosystem as a result of fire is reintroduced into the system from the atmosphere annually after a fire in equal annual amounts determined by dividing the total net N lost to the atmosphere during the most recent fire event by fire return interval (FRI). The FEM is implemented once annually if a fire is prescribed.

[10] The DOSM recalculates soil organic thickness after soil C pools are altered by ecological processes and fire disturbance based on the relationships between soil C content and soil organic thickness of different organic horizons in black spruce stands in Manitoba, Canada [*Yi et al.*, 2009b]. If the thickness of fibrous organic soil exceeds a specified threshold, the amount above the threshold is humified into amorphous soil. The specified thresholds for dry and wet black spruce ecosystems are 0.16 and 0.33 m, respectively. These values were determined as the mean plus one standard deviation of the fibrous organic horizon from a soil horizon data set compiled for numerous black spruce stands in Canada [*Yi et al.*, 2009b]. Once the thickness of each organic soil horizon (i.e., fibrous and amorphous) is determined, DOSM calculates the number of layers in each organic horizon and the thickness of each layer to maintain stability and efficiency of soil temperature and moisture calculations.

2.2. Model Calibration

[11] We developed a "dry" black spruce parameterizations for purposes of ultimately applying this parameterizations for a gradient of black spruce forest stands between well drained and intermediately drained landscape positions in interior Alaska [*Harden et al.*, 2003]. We also developed a "wet" black spruce parameterization for application to sites that are somewhat poorly and very poorly drained (i.e., with a high water table). To develop these parameterizations, we calibrated the rate-limiting parameters (maximum rate of C assimilation, respiration of vegetation per unit carbon at 0°C, C and N litterfall rate, maximum rate of N uptake by

Table 1. Target Pools and Fluxes Used for Calibration of the Dry and Wet Black Spruce Parameterizations of DOS-TEM in This Study[a]

	Dry	Wet
Vegetation carbon (gC/m^2)	4,000	3,250
Vegetation nitrogen (gN/m^2)	18.46	15.0
Soil carbon (gC/m^2)		
Fibrous	2,568	2,350
Amorphous	3,101	5,534
Mineral	10,447	12,377
Total	16,116	20,261
Soil organic nitrogen (gN/m^2)	542	741
Soil inorganic nitrogen (gN/m^2)	0.5	0.5
GPP ($gC/m^2/yr$)	745	593
NPP ($gC/m^2/yr$)	191	152
NPPSAT ($gC/m^2/yr$)	287	228
NUPTAKE ($gN/m^2/yr$)	2.30	1.83

[a]GPP, gross primary production; NPP, net primary production; NPPSAT, the saturation response of NPP to nitrogen fertilization; NUPTAKE, annual uptake of nitrogen from the soil.

vegetation, ratio between N immobilized and C respired by heterotrophs, heterotrohic repiration per unit carbon at 0°C for fibric, amorphous and mineral soil) of DOS-TEM for "target" values of pools and fluxes of mature "generalized" dry and wet black spruce stands based on estimates derived from studies conducted in Alaska and Manitoba and available in the literature (Table 1) as described below. The calibration of these parameters is an effective means of dealing with temporal scaling issues in ecosystem models [*Rastetter et al.*, 1992]. The data used for calibration generally did not involve data from Delta Junction because data from this location were used for model evaluation. The calibration process is similar to that used for previous versions of TEM [*Clein et al.*, 2002]. Because DOS-TEM represents three distinct soil C horizons (fibrous, amorphous, and mineral horizons), we determined a rate-limiting decomposition parameter for each of the horizons through calibration. The mean monthly climate data from Fairbanks (1901–1930) were used to drive the calibration.

[12] The target value for vegetation C in Table 1 was estimated by using measured aboveground live vegetation C, and the ratio between aboveground and total (both aboveground and belowground) live vegetation C. Published values of this ratio for black spruce stands range between 0.69 for black spruce stands of Ontario, Canada [*Chen et al.*, 2002] and 0.88 for black spruce stands of Saskatchewan, Canada [*Gower et al.*, 1997]. We used 0.8 in this study. The observed aboveground vegetation C for the dry black spruce parameterizations was based on the sum overstory tree C of mean dry black spruce stands of Alaska [*Vogel et al.*, 2008] and understory C from mature black spruce stands of Delta Junction, Alaska [*Mack et al.*, 2008]. We used the understory C from the Delta Junction sites used for evaluation because we could not find other estimates of understory C for black spruce stands in Alaska; the understory C from these sites was less than 5% of the aboveground biomass. For the wet black spruce stands, observed aboveground vegetation C was based on data presented by *Van Cleve et al.* [1983].

[13] Similar to vegetation C, the target value for net primary production (NPP) in Table 1 was estimated by dividing observed aboveground NPP by the fraction of aboveground NPP and total NPP. Published values of this fraction include 0.48 for black spruce stands of Ontario, Canada [*Chen et al.*, 2002], 0.4 to 0.6 for black spruce stands of Saskatchewan and Manitoba, Canada [*Gower et al.*, 1997], and 0.33 to 0.49 for black spruce stands of interior Alaska [*Ruess et al.*, 2003]. In this study, we used 0.43 as being representative of interior Alaska.

[14] The target values of soil C horizons (Table 1) were based on observed thickness of fibrous, amorphous and mineral layers and the drainage-dependent relationships between organic C content and organic horizon thickness from data compiled from Manitoba [*Yi et al.*, 2009b]. In Alaska, the observed thicknesses of fibrous and amorphous organic horizons are 10 and 6.5 cm for dry black spruce, and 13 and 13 cm for wet black spruce, respectively, based on field measurements of organic layers of mature black spruce stands of interior Alaska (M. R. Turetsky et al., A changing fire regime intensifies boreal burning, submitted to *Nature*, 2010). The N content of fibrous and amorphous horizons was estimated based on dividing the estimated C content of the horizons by C:N ratios. The C:N ratios of fibrous and amorphous horizons are 50 and 42 for dry black spruce, and 60 and 32 for wet black spruce, respectively, based on field measurements of black spruce stands in Manitoba, Canada [*Manies et al.*, 2005].

[15] The organic C content of the mineral soil was calculated based on drainage-dependent relationships between C density and depth below the mineral-organic interface [*Yi et al.*, 2009b]:

$$c_{den} = ae^{bh} + c_{\min} \tag{1}$$

where h is depth below the mineral-organic interface (cm), a and b are parameters fitted to the samples, and c_{min} is the minimum C density (gC/cm^3); c_{min} was assumed to be 0.0025 gC/cm^3 based on the soil C content between 1 and 2 m in mineral soil in the study of *Jobbagy and Jackson* [2000]; a and b are 0.03969 and 0.06674 for the dry black spruce parameterization, and 0.04856 and 0.06164 for the wet black spruce parameterization, respectively. These coefficients were derived by fitting the relationship to measurements from Manitoba, Canada [*Manies et al.*, 2006; J. Harden, unpublished data, 2010]. Similarly, we estimated the organic N content of the mineral horizon by dividing the C content by the C:N ratio of the mineral horizon. The C:N ratios of the mineral horizon are 26.3 and 23.7 for the dry and wet black spruce parameterizations, respectively. The target value for the total organic N in the soil (SOLN) is the sum of the N content of the fibric, amorphous, and mineral horizons. All the other target values in Table 1 were estimated as described by *Clein et al.* [2002].

2.3. Model Evaluation

[16] To assess the ability of DOS-TEM to simulate the structure of organic soils in black spruce forest ecosystems, we evaluated the dry black spruce parameterization of the DOS-TEM at two sites with well drained soils with no permafrost and two sites with intermediately drained soils with permafrost; all sites are located near Delta Junction, Alaska (65°53′N, 145°44′W). The well-drained sites are the Donnelly Flats tower control site (DFTC), which last burned around 1921 and the Donnelly Flats tower burn site (DFTB),

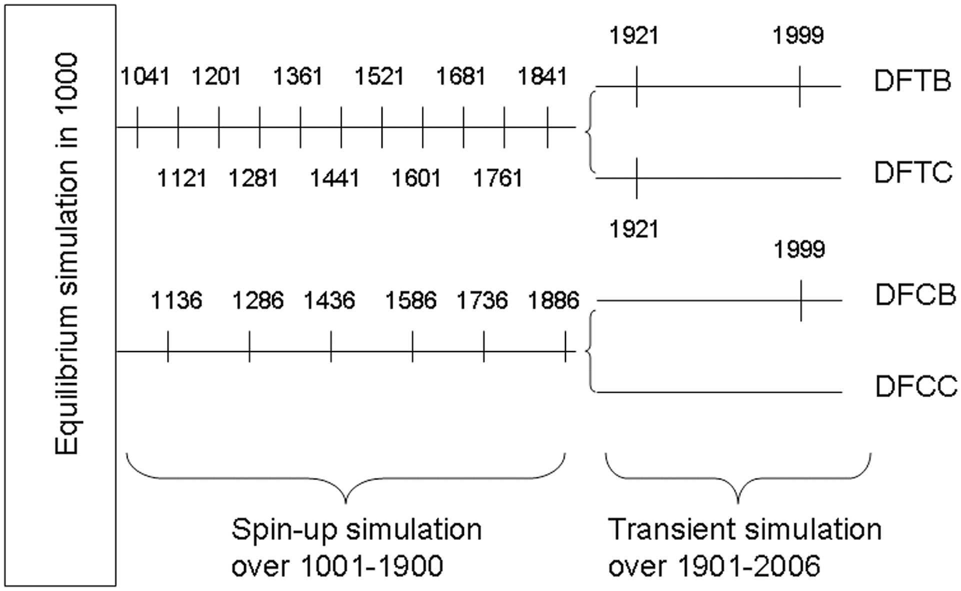

Figure 4. The protocol for the simulation of carbon and nitrogen dynamics for the four sites in Delta Junction, Alaska, near well drained and intermediately drained chronosequences: Donnelly Flats Tower Control (DFTC), Donnelly Flats Tower Burn (DFTB), Donnelly Flats Creek Control (DFCC), and Donnelly Flats Creek Burn (DFCB). All simulations start from an equilibrium condition in year 1000. The values with vertical bars show the year of fire event either derived from field studies or from back-casting from the latest known burn.

which burned in 1999 [*Liu and Randerson*, 2008]. The intermediately drained sites are the Donnelly Flats Creek Control site (DFCC), which last burned around 1886, and the Donnelly Flats Creek burn site (DFCB), which burned in 1999. For more information on the soil and vegetation data of these sites, see *Harden et al.* [2006], *Mack et al.* [2008], *Manies et al.* [2005], and *Yi et al.* [2009a, 2009b]. We did not evaluate the wet black spruce parameterization in the same manner as the dry black spruce parameterization because there have not been any studies conducted in interior Alaska that would allow us to evaluate the effects of fire on the reaccumulation of organic matter.

[17] The application of the model was driven by monthly climate data, which included air temperature, precipitation, vapor pressure, and surface solar radiation, that were retrieved from the Climate Research Unit (CRU) data sets [*Mitchell and Jones*, 2005] for the period 1901–2002. The CRU data sets do not include the period 2003–2006, so the anomalies of the National Center for Environmental Prediction (NCEP) reanalysis data sets [*Kanamitsu et al.*, 2002] were used to extend CRU data sets through 2006 [*Hayes et al.*, 2010]. We modified this CRU/reanalysis data set by replacing the temperature and precipitation data with data from meteorological stations of Delta Junction (from 1941 to 2006) and Fairbanks (from 1930 to 2006). The atmospheric CO_2 data used to drive the simulations were obtained from the Mauna Loa station [*Keeling and Whorf*, 2005].

[18] The implementation of fire in the simulations we conducted, which treated these sites as self-replacing black spruce stands, is described in Figure 4. We initially ran DOS-TEM to equilibrium in year 1000, using mean monthly climate of 1901–1930 for Delta Junction. The simulation from year 1001 to 1900 was driven with mean monthly climate of the 1901–1930 time period repeated every 30 years throughout that portion of the simulation. Fire disturbances were backcast prior to the earliest known fire event based on FRI, which we assumed to be 80 years at DFTC and DFTB and 150 years at DFCC and DFCB based on the similar landscapes in Manitoba (B. J. Stocks, personal communication, 1997). Although we do not have data from interior Alaska that allows us to better estimate the FRI of well drained and intermediately drained black spruce sites in interior Alaska, a recent study estimates that FRI in interior Alaska was 159 years between 1860 and 1919 and has decreased to 105 years between 1920 and 2009 [*Kasischke et al.*, 2010]. These estimates suggest that our estimates of 80 and 150 years for well drained and intermediately drained black spruce sites are reasonable. Finally, we ran the model over the 1901–2006 time period driven monthly climate from the modified CRU/reanalysis data set.

[19] We performed two sets of simulations, one used the DOSM (i.e., with dynamic organic soil, DOS) versus others that kept organic soil thickness static (SOS). For DOS simulations, organic soil thickness is changed at the time of fire disturbance and during postfire succession. In the SOS simulations, C pools are reduced at the time of fire disturbance, but the thickness of organic soil is not changed.

[20] We compared the simulated (with DOS and with SOS) thickness of organic soil, and C of organic soil and mineral soil with measurements made at the four sites in year 2001 [*Harden et al.*, 2006]. The deepest measurement of C in mineral soil at DFTC was 82 cm, at DFTB was 67 cm, at DFCC was 22 cm, and at DFCB was 35 cm. We also compared the outputs over the 1001–1900 period to evaluate differences between the DOS and SOS simulations.

Table 2. Comparisons Between Simulated and Measured Estimates of Organic Soil Thickness, Carbon Content in Organic Soils, and Carbon Content in Mineral Soils at Four Sites near Delta Junction, Alaska, in Well Drained and Intermediately Drained Chronosequences[a]

	DFTC	DFTB	DFCC	DFCB
	Organic Layer Thickness (cm)			
Measured	10.4 (6.2)	5.2 (3.2)	19.0 (3.0)	10.0 (3.5)
Modeled				
DOS	13.7	7.7	19.9	12.1
SOS	22.8	22.8	22.8	22.8
	Organic Soil Carbon Content (gC/m^2)			
Measured	2,866 (1,502)	2,196 (1,870)	5,447 (3,594)	4,676 (1,101)
Modeled				
DOS	3,047	2,036	5,601	3,963
SOS	3,824	2,135	5,636	4,023
	Mineral Soil Carbon Content (gC/m^2)			
Measured	5,276 (427)	4,964 (1681)	6,405 (n/a)	6,957 (n/a)
Depths of sampled mineral soil (cm)	50, 55,82	48, 55, 62, 65, 67	22	35
Modeled				
DOS	8,143	8,315	8,675	8,707
SOS	13,767	13,888	13,798	13,819

[a]Modeled: DOS, for model simulations with dynamic organic soil; SOS, for model simulations with static organic soil. Measured: mean (standard deviation). DFTC, Donnelly Flats Tower Control; DFTB, Donnelly Flats Tower Burn; DFCC, Donnelly Flats Creek Control; DFCB, Donnelly Flats Creek Burn. The measurements were obtained in 2001. The depths of sampled mineral soil for carbon estimates of the mineral soil are also provided. See *Harden et al.* [2006] for more information on the measurements and estimates.

2.4. Model Sensitivity Analyses Involving Soil Drainage and Fire Return Interval

[21] Our goal in developing DOS-TEM is to better represent and understand the effects of fire on soil C dynamics of forests in boreal regions. There are two important factors that control the spatial heterogeneity of soil C responses to fire in boreal forests: soil drainage and fire frequency. We conducted simulations with DOS-TEM to understand the sensitivity of ecosystem C dynamics to these factors. All simulations in these sensitivity analyses were driven by Delta Junction climate from year 1001 through 1900.

[22] To evaluate the sensitivity of C dynamics to soil moisture as it is influenced by depth to permafrost and soil drainage class, we performed two sets of simulations: (1) a simulation for the dry black spruce parameterization with FRI of 100 years and moderate belowground burn severity (69% organic soil depth; see Table C1), and (2) simulations of the wet black spruce parameterization with FRI of 100 and 200 years. FRIs of 100 and 200 years are appropriate for dry and wet black spruce sites in interior Alaska, respectively. The simulation of the wet black spruce parameterization with FRI of 100 years was conducted to separate out the effects of drainage versus FRI in comparing the dynamics of the dry and wet black spruce parameterizations.

[23] To evaluate the sensitivity of C dynamics to fire frequency, we performed three simulations using the dry black spruce parameterization with FRIs of 150, 100, and 60 years, all with moderate belowground burn severity (69% of the organic soil depth was combusted; also see Table C1).

3. Results

3.1. Evaluation

[24] The organic layer thicknesses of DOS simulations (i.e., the simulations with dynamic organic soil structure) were all within 1 standard deviation of the mean of the measurements at all 4 sites, while those of SOS simulations (i.e., the simulations with static organic soil structure) were kept at 22.8 cm (Table 2). The estimated C of organic soils in both the DOS and SOS simulations were within 1 standard deviation of the mean of the measurements at all 4 sites. Differences in the estimates of C in the mineral soil between the DOS and SOS simulations were large; C estimates in the mineral soil of the SOS simulations were approximately 70% larger than those in the DOS simulations.

[25] During the spin up portion of the simulation, the organic soil thickness of the DOS simulations were reduced abruptly at the occurrence of a fire, and recovered during succession. In comparison to the SOS simulation, this change in organic soil thickness caused differences in soil environmental conditions and carbon dynamics (Figure 5). At the occurrence of fire in both the DOS and SOS simulations, vegetation C, net primary production (NPP), organic soil C, and heterotrophic respiration (RH) decreased immediately. Because of the change in organic soil thickness, the active layer depth in the DOS simulation increased, as did water table depth, which increased in response to enhanced drainage associated with the deepening of the active layer. In contrast, the active layer depth of the SOS simulation increased slightly, and there was very little variation in water table depth. The RH of DOS simulation increased immediately due to warmer soil conditions, while the RH of the SOS simulation remained low because of the cold wet soil conditions.

[26] The RH of the DOS simulation kept decreasing until approximately 50 years after fire as both organic and mineral soil C stocks dropped because of the negative carbon balance (RH greater than NPP). After 50 years, the RH of the DOS simulation started to increase as both organic and mineral soil C increased as the soil became colder and the ecosystem transitioned into positive carbon balance. In contrast, RH of the SOS simulation continually increased after fire because of continual increases in organic soil C associated with positive carbon balance of the cold wet soil. The increase in RH in the SOS simulation versus the decrease in RH in the DOS simulation in the decades following fire causes net nitrogen mineralization to increase faster in the SOS simulation, which caused NPP and vegetation C to increase more quickly during succession than in the DOS simulation.

[27] The thickness of the organic soil in the DOS simulations increased to preburn levels approximately 80 years after fire. During succession, the active layer depth of the DOS simulation continually decreased while the water table depth stabilized after about 40 years. NPP and vegetation C in both the DOS and SOS simulations reached a maximum approximately 30 and 70 years after fire, respectively. The maximum NPP and vegetation C of SOS simulation were

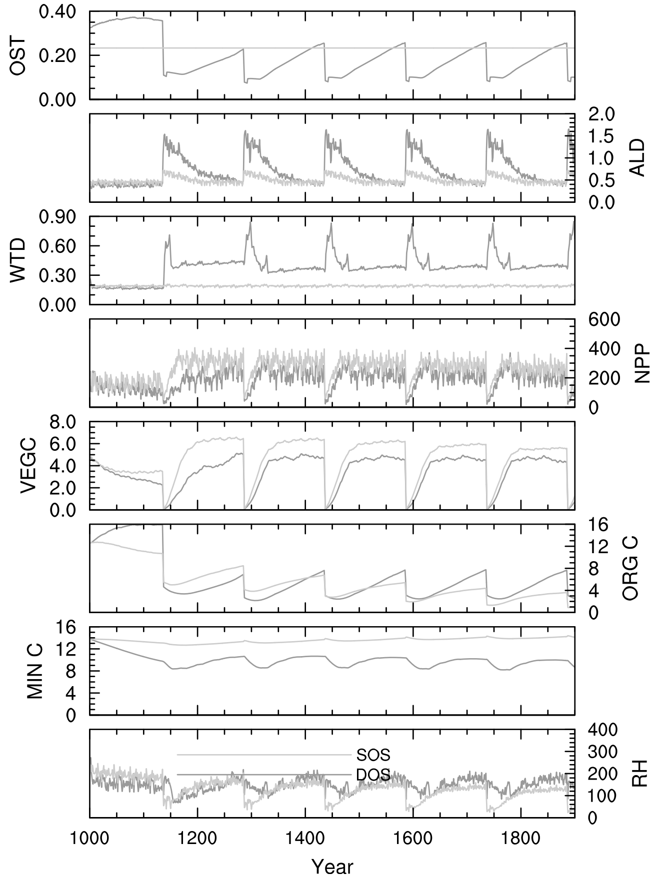

Figure 5. Comparisons of various aspects of ecosystem dynamics between the application of DOS-TEM with a dynamic organic soil (DOS) and a static organic soil (SOS) for a site typical of the intermediately drained sites near Delta Junction (Donnelly Flats Creek Control and Burn sites) w ith a 150 year fire return interval. Variables compared include organic soil thickness (OST; m), active layer depth (ALD; m), water table depth (WTD; m), available nitrogen (AVLN; gN/m^2), net primary production (NPP; gC/m^2/yr), vegetation carbon (VEGC), organic soil carbon (ORGC; kgC/m^2), mineral soil carbon (MIN C; kgC/m^2) and heterotrophic respiration (RH; gC/m^2/yr).

always greater than those of DOS simulation. The C in mineral soil of SOS simulation was approximately 5 kgC/m^2 greater than that of DOS, due to colder soil temperature.

3.2. Sensitivity Analyses

3.2.1. Effects of Drainage

[28] For all simulations in the drainage sensitivity analysis, the thickness of organic soil, NPP, vegetation C, and organic soil C declined immediately at the time of fire disturbance, and the active layer depth, water table depth, and RH increased (Figure 6). During succession, all these variables almost recovered to prefire states. The water table depth of dry drainage simulation was large (about 0.8 m after fire, and 0.4 m before fire), while the water table depth of the wet drainage simulations was small. The maximum NPP of dry drainage simulations was greater that those of the wet drainage simulations. The vegetation C of dry drainage simulation reached a maximum (~5.0 kgC/m^2) after about 50 years, while for vegetation Cs of wet drainage simulations did not reach a maximum (~4 kgC/m^2) until after 70 years. The organic soil C of dry drainage simulation was consistently smaller than those of wet drainage simulations, due to higher fire severity defined for dry drainage simulation. The mineral soil C of dry drainage simulation was consistently greater than those of wet drainage simulations. This occurred because the litter input of C into the soil is based on a static fine root distribution, so that when the organic soil thickness of the dry drainage simulation is smaller, then more litter fall is input into the mineral soil.

3.2.2. Effects of Fire Frequency

[29] For both wet (Figure 6) and dry (Figure 7) drainage conditions, the simulations with longer fire return interval (FRI) had thicker organic soils and more organic soil C storage. For the wet drainage simulations, the longer FRI simulation had less mineral soil C. In contrast, the 150 and 100 year FRI simulations for the dry drainage calibration had more mineral soil C than the 60 year FRI simulation; the

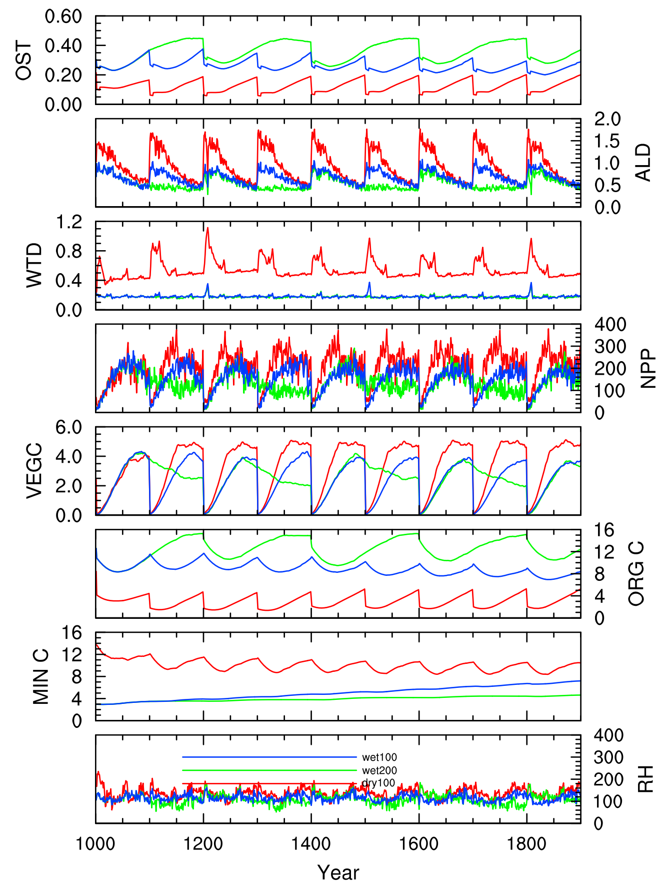

Figure 6. Comparisons of various aspects of ecosystem dynamics between the application of DOS-TEM for wet (wet100, with 100 year fire return interval; wet200, with 200 year fire return interval) and dry (with 100 year fire return interval) black spruce parameterizations. Variables compared include organic soil thickness (OST; m), active layer depth (ALD; m), water table depth (WTD; m), net primary production (NPP; gC/m^2/yr), vegetation carbon (VEGC), organic soil carbon (ORG C; kgC/m^2), mineral soil carbon (MIN C; kgC/m^2), and heterotrophic respiration (RH; gC/m^2/yr).

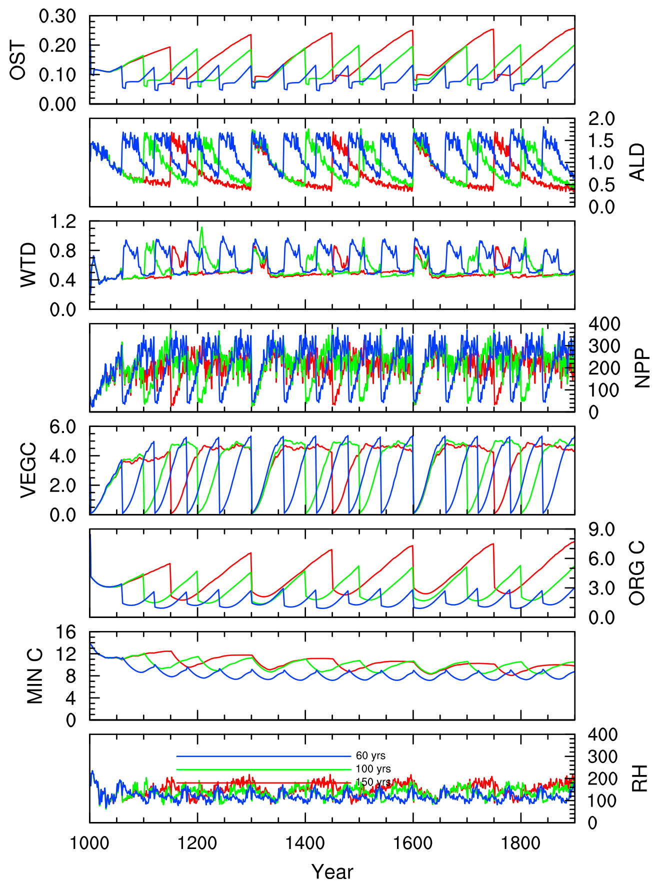

Figure 7. Comparisons of various aspects of ecosystem dynamics among the application of DOS-TEM for fire return intervals of 60, 100, and 150 years. Variables compared include organic soil thickness (OST; m), active layer depth (ALD; m), water table depth (WTD; m), net primary production (NPP; gC/m^2/yr), vegetation carbon (VEGC), organic soil carbon (ORG C; kgC/m^2), mineral soil carbon (MIN C; kgC/m^2), and heterotrophic respiration (RH; gC/m^2/yr).

difference between 150 and 100 year FRI simulations was small. For both dry and wet drainage simulations, the prefire NPP for the shorter FRI simulation tended to be greater than that of the longer FRI simulation. The colder soil environment in the longer FRI simulations led to lower NPP just before the fire. For example, the active layer of the 150 year FRI simulation was ~40 cm shallower than that of 60 yr FRI simulation.

4. Discussion

4.1. Importance of Dynamic Organic Soil to Ecosystem Dynamics

[30] Both soil temperature and moisture are important drivers of ecosystem dynamics in northern high-latitude ecosystems [*Yi et al.*, 2009a]. This study has taken a new approach of explicitly coupling soil organic C dynamics with the dynamics of soil organic horizon thicknesses in order to explicitly represent the dynamic linkage between biogeochemical and soil environmental processes in northern high-latitude ecosystems. In dry black spruce ecosystems, the reduction of the organic layer thickness causes an increase in active layer depth and subsurface drainage, which in the soils parameterized in this study results in a transient/temporary decrease in soil moisture. Our analysis of differences between dynamic organic soil simulation and the static organic soil simulation indicated that mineral soil carbon storage is substantially and unrealistically higher if the dynamics of the organic soil horizons are not explicitly represented.

4.2. Interactions Between Soil Environment and Ecosystem Dynamics

[31] Soil temperature is considered to be one of the most important environmental factors affecting soil C decomposition and nutrient availability to plants [*Davidson and Janssens*, 2006]. In our simulations, both the active layer depth and available N increased immediately after fire in both dry and wet black spruce ecosystems. However, in mid succession, both active layer depth and available N tended to decrease as organic matter accumulated. NPP and vegetation C tended to reach maxima in mid succession, after which NPP tended to decline while vegetation C either stabilized (in dry black spruce ecosystems) or declined (in wet black spruce ecosystems). Age–related declines in forest productivity have received substantial attention in the forest science literature [*Gower et al.*, 1996; *Goulden et al.*, 2010]. Several studies have hypothesized that the accumulation of a thick organic layer, which contributes to soil cooling and reduction of nutrient availability, may, in part, be responsible for declines in productivity as forest stands age [*Prescott et al.*, 2000; *Simard et al.*, 2007]. In our simulations, these hypotheses are supported by an accumulation of organic soil and canopy development after fire disturbance that caused soils to get colder and restrict the availability of soil inorganic N, which then decreased NPP.

[32] Water table depth is also an important control on soil C decomposition and nutrient availability [*Funk et al.*, 1994; *Dunn et al.*, 2007]. In our simulations there tended to be an increase in water table depth from ~0.4 to ~0.8 m in dry black spruce ecosystems after fire associated with the decrease in the thickness of organic horizons and the increase in active layer depth. In contrast, the simulated water table depth in the wet black spruce ecosystems remained relatively stable in association with a stable thickness of the organic soil over the 900 year simulation period. This relationship between organic soil thickness and water table depth is important. As discussed by *Yi et al.* [2009a], leaf area changes had relatively little impact on soil water dynamics in comparison with the effects of changes in the thickness of organic soil horizons on active layer depth and subsurface drainage.

4.3. Role of Soil Drainage on Ecosystem Dynamics

[33] Drainage is an important control on the C dynamics of black spruce ecosystems [*O'Connell et al.*, 2003; *Grant*, 2004; *Harden et al.*, 2000] because of its effects on NPP, decomposition rates, and fire frequency. In our study, we developed generalized parameterizations for dry and wet black spruce ecosystems. In general, wet black spruce ecosystems have thicker organic soils, more soil C storage, less vegetation C, and lower NPP than dry black spruce ecosystems. Our model successfully simulated these differences.

4.4. Role of Fire Frequency on Ecosystem Dynamics

[34] The frequency of fire is important in regulating the size of soil C pools in black spruce ecosystems [*Harden et al.*, 2000]. As expected, simulations in our study with longer FRI (e.g., 150 years) had thicker organic horizons (higher soil C content) than simulations with shorter FRI (e.g., 60 years). FRI also affects plant productivity. Simulations with longer FRI tended to have lower NPP before fire disturbance (e.g., see the 150 year FRI simulation in Figure 7 and the 200 year FRI simulation in Figure 6). As discussed earlier, a thicker organic soil in older ecosystems causes a colder soil environment and restricts nutrient availability to plants.

4.5. Uncertainties and Limitations

[35] We simulated the dynamics of organic soil based on relationships between organic soil thickness and soil C from black spruce stands in Manitoba, Canada [*Yi et al.*, 2009b]. However, it is not clear to what degree these relationships hold true for black spruce ecosystems in Alaska. Future studies should also develop similar relationships for other forest ecosystems in Alaska, particularly for successional forests after fire. The soil C simulated in DOS-TEM represents soil C in three horizons (fibrous, amorphous and mineral soil C), and these horizons are further divided into layers for the efficient computation of soil thermal and hydrological dynamics. Therefore, each soil layer, which represents an explicit pool of soil C tracked by the model, has a decomposability that is typical of either fibrous, amorphous, or mineral soil C horizons that is implemented through the rate-limiting parameter for decomposition for that horizon. Thus, the model considers multiple pools of soil C in which the decomposability of the soil C is vertically stratified in the soil. It may prove useful to represent each soil C layer by multiple pools similar to that represented in CENTURY model [*Parton et al.*, 1987]. However, approaches to date that have implemented both one and multiple pools for each layer in organic soils of black spruce ecosystems have not shown an overwhelming improvement in representing soil C dynamics with multiple pools within each soil layer [*Carrasco et al.*, 2006; *Fan et al.*, 2008]. It is our opinion that most of the variability in the decomposability of soil C in black spruce ecosystems is explained by depth in the soil, and that a vertical differentiation of soil C quality is appropriate for these ecosystems.

[36] Another uncertainty is associated with parameters used in the model that have the potential to change during succession. After fire disturbance, the effect of canopy development on ground temperature was simulated using the N factor approach [*Klene et al.*, 2001; *Karunaratne and Burn*, 2004], which specifies surface ground temperature as a ratio with respect to 2 m air temperature. In this study, N factor varied from 1.1 immediately after a fire to 0.69 after 70 years. Vertical root distribution is another factor that may change during succession. In our implementation, the vertical root distribution was assumed to be static at all stages of ecosystem development after fire. Clearly, a better empirical understanding of the time course of N factor and vertical root distribution would be useful for better representing the influence of these factors on ecosystem dynamics.

[37] In modeling the impacts of fire on C cycling, knowledge of factors that control both fire frequency and fire severity at landscape scales are needed. Currently, spatial variations in fire frequency are assigned at very coarse resolutions (e.g., 0.5 by 0.5 degrees [*Balshi et al.*, 2007]), but studies show that actual susceptibility to burning at the landscape scale is controlled by vegetation type, topography, and weather at the time of the fire event [*Renkin and Despain*, 1992; *Bessie and Johnson*, 1995; *Cumming*, 2001]. As more information on factors that control the spatial patterns of burning in black spruce forests becomes available, a more realistic depiction of fire frequency can be incorporated into DOS-TEM. Along a similar vein, results from recent research has also provided a clearer understanding of a number of factors that control depth of burning in black spruce forests, including fire frequency, fire year size, timing of the fire during the growing season, and topography [*Kasischke and Johnstone*, 2005; *Johnstone*, 2006; *Kane et al.*, 2007; Turetsky et al., submitted manuscript, 2010]. In our implementation of DOS-TEM in this study, we primarily used a look-up table approach that largely depended on fire season, annual area burned in Alaska, and soil drainage to define the burn severity of soil organic horizons. More sophisticated decision rules that better describe the temporal and spatial variability of burn severity need to be developed and incorporated into DOS-TEM as our understanding of the heterogeneity of burn severity improves. It is also our intention to make better use of the effects of soil environmental variability on the combustion of soil organic horizons as our understanding of this linkage improves.

5. Conclusion

[38] In this paper, we presented and evaluated a dynamic organic soil version of TEM for studying the effects of fire on soil temperature, moisture, and ecosystem dynamics. The model represents the dynamic linkage among soil organic thickness, soil C content, and soil environmental conditions. Our analyses in this study have shown that it is important to represent this dynamic linkage. Our analyses also indicate that landscape variability in fire frequency and drainage should be considered in large-scale applications of the model. As fire frequency and fire severity are presumably related to soil drainage, it is important to articulate these linkages in future spatial applications of the model as our understanding of these linkages improves.

[39] The dynamic organic soil version of TEM (DOS-TEM) directly evolved from the version of TEM used by *Balshi et al.* [2007, 2009a] to study the role of fire in the C dynamics of northern high latitudes. There are four parts in DOS-TEM: the environmental module (EnvM), the ecological module (EcoM), the fire effects module (FEM), and the dynamic organic soil module (DOSM). The detailed description of EnvM was provided in the appendix of *Yi et al.* [2009a]. Here, we provided an overview of of EnvM (Appendix A), and detailed descriptions of EcoM (Appendix B), FEM (Appendix C), and DOSM (Appendix D).

Appendix A: Environmental Module

[40] The environmental module EnvM operates at a daily time step using daily air temperature, vapor pressure, surface solar radiation and precipitation, which are downscaled from

monthly input data. The EnvM considers the radiation and water fluxes among the atmosphere, canopy, snowpack and soil. Live moss and fibrous and amorphous organic horizons are considered in the soil column in addition to a mineral soil horizon. Soil moisture and temperature are updated at daily time step. A Two-Directional Stefan Algorithm is used to predict the positions of freezing/thawing fronts in the soil. The temperature of soil layers above first freezing/thawing front and below the last freezing/thawing front is updated separately by solving finite difference equations. Temperatures of the soil layers between the first and last freezing/thawing fronts are assumed to be at the freezing point. Soil moistures are only updated for unfrozen layers by solving Richard equation. Both the thermal and hydraulic properties of soil layers are affected by its water content. The simulated estimates of daily evapotranspiration, soil temperature and moisture are integrated to monthly values, and provided to EcoM. See *Yi et al.* [2009a] for more details on the EnvM and an evaluation of the performance of the soil temperature and moisture simulations by the module.

[41] For application in this study, we found it necessary to modify the mineral soil structure of the EnvM described by *Yi et al.* [2009a], in which there were 5 mineral soil layers with thicknesses from top to bottom of 0.1, 0.2, 0.5, 1 and 2 m. In this study, to improve the simulation of soil water dynamics, we used 13 mineral soil layers in the following order from top to bottom: four with thicknesses of 0.1 m, three with thicknesses of 0.2 m, three with thicknesses of 0.3 m, and single layers with thicknesses of 0.5 m, 1 m, and 2 m.

Appendix B: Ecological Module

[42] The detailed description on the ecological processes of TEM have largely been documented in previous studies [*Raich et al.*, 1991; *McGuire et al.*, 1992; *Tian et al.*, 1999; *Zhuang et al.*, 2003; *Euskirchen et al.*, 2006]. In this study, we only provided descriptions of new implementations in the model. Section B1 describes the usage of freezing/thawing fronts to determine the start and end of photosynthesis. Section B2 describes the detailed implementation of vertical soil C dynamics, and section B3 provides a detailed description of woody debris dynamics.

[43] The ecological module EcoM operates at monthly time step driven by monthly atmospheric climate input data and simulated environmental data. Monthly leaf area index (LAI) is estimated in EcoM, and provided to EnvM at end of each month. The fibrous and amorphous organic horizon thicknesses are updated at the end of each year, based on the simulated soil C in each horizon. The thicknesses of organic horizons are provided to DOSM.

B1. Gross Primary Production

[44] Gross primary production (GPP) is calculated at a monthly time step and is affected by several factors [*Zhuang et al.*, 2003]:

$$GPP = C_{\max} f(PAR) f(PHENOLOGY) f(FOLIAGE) f(T) \cdot f(C_a, G_v) f(NA) f(FT) \quad \text{(B1)}$$

where $C_{\max}$ is the maximum rate of C assimilation; *PAR* is photosynthetically active radiation, $f(PHENOLOGY)$ is monthly leaf area relative to leaf area during the month of maximum leaf area; $f(FOLIAGE)$ represents the ratio of canopy leaf biomass relative to maximum leaf biomass; $f(T)$ represents the effect of air temperature; C_a and G_v are atmospheric CO_2 concentration and relative canopy conductance, respectively, $f(C_a, G_v)$ represents the effect of stomatal regulation on atmospheric CO_2 uptake; $f(NA)$ represents the limiting effect of available inorganic N on GPP; and $f(FT)$ represents the effect of freeze and thaw on photosynthetic activity. Except for $C_{\max}$, other factors in equation (B1) all range from 0 to 1.

[45] In the work of *Zhuang et al.* [2003], 10 cm soil temperatures (°C) of the previous, current, and next month were used to calculate $f(FT)$. Based on the signs of temperatures of the three months (greater or less than the freezing point), 8 categories of monthly freeze and thaw status are possible. For each of these 8 categories, a different equation is used to calculate $f(FT)$. In this study, the positions of the freezing and thawing fronts are used to calculate a daily $f(FT)$. It is assumed that if the thawing front penetrates 5 cm of the soil column (excluding living moss), then $f(FT)$ of that day is 1, otherwise it is 0. The monthly value $f(FT)$ is calculated as the mean of the daily values.

B2. Litter Input and Soil Carbon Dynamics

[46] As in previous versions of TEM, soil C balance can be described as the difference between litter input to the soil and soil C decomposition. Different from previous version of TEM, C litter input is divided into aboveground litterfall and belowground litterfall. Aboveground litterfall is assigned only to the first soil layer, while belowground litterfall is assigned to different soil layers based on fractional distribution of fine roots with depth. We assume that the ratio of aboveground litterfall to total litter input is similar to the ratio of root NPP to total NPP. Studies estimate that root NPP contributes approximately 40–60% of total NPP for black spruce in the boreal forest of North America [*Steele et al.*, 1997; *Ruess et al.*, 2003]. In this study, we set the ratio between aboveground litterfall and total litter input at 0.43 of based on the ratio of aboveground NPP to total NPP that has been estimated for of Alaska black spruce (R. W. Ruess, unpublished data, 2010).

[47] Soil C is tracked in the fibrous, amorphous, and mineral horizons in DOS-TEM, and soil C decomposition for each layer within a soil horizon is calculated based on the soil environmental conditions of that layer:

$$R_{H,i} = K_{d,i} C_{s,i} f(M_{v,i}) f(T_{s,i}) \quad \text{(B2)}$$

where i is soil layer index, $R_{H,i}$ is heterotrophic respiration from layer i ($gC/(m^2mon)$), $K_{d,i}$ is heterotrophic respiration rate at 0 °C of layer i ($gC/(m^2mon)$), $C_{s,i}$ is soil C storage in layer i (gC/m^2), and $f(M_{v,i})$ and $f(T_{s,i})$ are moisture and temperature factors affecting decomposition of layer i. $f(M_{v,i})$ is parabolic relationship using the predefined parameters for the maximum, minimum, and optimal volumetric soil moisture for decomposition, which are 1, 0, and 0.5, respectively. When simulated volumetric soil moisture equals 0.5, $f(M_{v,i})$ equals 1. $f(T_{s,i})$ is calculated based on a Q_{10} (2.0 in this study) and soil temperature of layer i. There is a unique rate limiting parameter for decomposition K_d for the fibrous, amorphous, and mineral soil horizons, that is used to estimate decompo-

Table C1. The Fire Severity Category, Fraction of Aboveground Vegetation Biomass, and Soil Organic Horizons (Moss, Fibrous, and Amorphous) Combusted During a Fire Based on the Type of Soil Drainage, the Season of Burning, and the Relative Area Burned in a Particular Year

Soil Drainage	Fire Season	Relative Area Burned	Fire Severity Category	Relative Amount of Aboveground Vegetation Biomass Consumed[a]	Relative Amount of Organic Soil Consumed by Depth[b]
Dry	early	small	low	0.16	0.54
		large to ultralarge	moderate	0.24	0.69
	late	all sizes	high	0.32	0.80
Wet	all seasons	all sizes	NA	0.16	0.48

[a]Based on *French et al.* [2002].
[b]Based on E. Kasischke (unpublished data, 2010).

sition for each layer within the horizon. The rate limiting parameter is determined by calibrating the model to target values for the C content of the three organic horizons.

B3. Woody Debris

[48] Woody debris C and N dynamics were included in DOS-TEM. Woody debris originates from aboveground dead vegetation. After fire disturbance, dead aboveground vegetation is completely converted to wood debris in 9 years based on *Manies et al.* [2005]. The rate limiting parameter for decomposition K_d of wood debris is assumed to be the same as that for the amorphous organic horizon. The soil temperature and moisture of first organic layer are used to drive decomposition of wood debris (see equation (B2)).

Appendix C: Fire Effects Module

C1. Combustion of Vegetation

[49] At a fire event, aboveground vegetation C and N is divided into 3 components: combusted (a percentage of prefire aboveground vegetation biomass), aboveground dead (a percentage of prefire aboveground vegetation biomass) and aboveground live (1% of prefire aboveground vegetation biomass). The percentage of prefire above biomass combusted is determined from Table C1, e.g., 16% in dry black spruce ecosystems in small fire years. The percentage of prefire aboveground biomass that is dead is then calculated as the residual fraction after accounting for the combusted biomass and the aboveground live biomass. The belowground vegetation C is also divided into 3 components: combusted (belowground vegetation biomass from the surface to the depth of burn), belowground live (1% of prefire belowground vegetation biomass), and belowground dead (all remaining belowground vegetation biomass).

C2. Combustion of Surface Soil Organic Layers

[50] The FEM calculates an index of burn severity that ranges from 0 to 1, based on the fire season, area burned in Alaska, and soil drainage (Table C1). Fire season is broadly classified into two categories: early season (July and months before July), and late season (August and months after August). The area burned in Alaska is broadly classified into four categories: small fire years (less than 1% of interior Alaska), large fire years (1–2% of interior Alaska burned), very large fire years (2–3% of interior Alaska burned), and ultralarge fire years (>3% of interior Alaska burned). The relative amount of area burned is determined through analysis of records for area burned in Alaska between 1950 and 2006 [*Kasischke et al.*, 2010]. For application of the model to years before 1950, the influence of area burned on burn severity is generated randomly. The depth of burn of the surface organic soil is then calculated by multiplying burn severity from Table C1 by the total thickness of the moss, fibrous, and amorphous horizons in the soil column.

[51] Based on the calculated depth of burn, the soil C in the combusted layers is emitted to atmosphere. The dead belowground vegetation C is assigned to each of the remaining soil layers based on the distribution of fine root biomass in those soil layers. Similarly the fraction of N is combusted and emitted to atmosphere and dead vegetation N is assigned to soil organic N.

C3. Retention and Reinput of Nitrogen

[52] The combusted N from both vegetation and organic soil are divided into two components: (1) N volatized into atmosphere and (2) N retained in ecosystem. It is assumed that 85% of combusted N is retained based on *Harden et al.* [2004]. The volatized N is then reinput into the ecosystem in equal annual amendments in subsequent years based on dividing the volatilized N by the FRI.

Appendix D: Dynamic Organic Soil Module

[53] DOSM updates the organic soil structure at the time of fire and at the end of each year, based soil C content of the fibrous and amorphous horizons. DOSM is important in defining the structure of soil organic horizons for the purpose of maintaining the stability and efficiency of soil temperature and moisture calculations when thickness of organic soil C is altered by either wildfire disturbance or ecological processes. The soil organic structure consists of a maximum of 1 moss layer, 3 fibrous organic layers, and 3 amorphous organic layers. It is assumed that the minimum soil layer thickness for each horizon is 2 cm. If the thickness of a layer is less than 2 cm, a layer will be combined with other layers of the same horizon, or be reset to 2 cm if there is only one layer for a horizon (except for live moss, which will not be included in the soil column if it is less than 2 cm). The rationale behind the assignment of the organic soil layer thickness is that the upper layers in the soil column should be thinner than deeper layers, following the common practice of land surface models and ecosystem models in simulation soil thermal and

Table D1. The Configuration of Soil Layers Within the Fibrous Organic Horizon, Based on Total Organic Thicknesses (cm)

Total Thickness (DZ)	Layer 1 (Top)	Layer 2	Layer 3
0~4	DZ (> = 2)		
4~6	2	DZ-2	
6~10	3	DZ-3	
10~15	2	4	DZ-6
15~20	3	6	DZ-9
20~28	4	8	DZ-12
28~33	5	10	DZ-15

moisture dynamics. At the same time, the upper layer should not so thin that it leads to instability and inefficiency in calculations of soil thermal and moisture dynamics. The assignment of layer thickness for the fibrous organic horizon is provided in Table D1. The thicknesses and number of layers in the amorphous organic horizon (n_{amp}) are based the thickness of deepest fibrous horizon layer ($d_{fib,bot}$) and the total thickness of amorphous organic horizon (d_{amp}).

$$n_{amp} = \begin{cases} 1 & d_{amp} < 3d_{fib,bot} \\ 2 & 3d_{fib,bot} \leq d_{amp} < 6d_{fib,bot} \\ 3 & d_{amp} \geq 6d_{fib,bot} \end{cases} \quad \text{(D1)}$$

Then, (1) if there are 2 layers with the amorphous horizon, the thicknesses of them are 1/3 and 2/3 of amorphous organic horizon thickness, respectively; (2) if there are 3 layers, the thicknesses of them are 1/6, 2/6, and 3/6 of the amorphous organic horizon thickness, respectively.

[54] At the beginning of each year, the thicknesses of the moss layer, fibrous organic layers, and amorphous organic layers are checked. If any of these layers have thickness less than minimum value, or if the total thickness and total number of fibrous layers are not consistent with those in Table D1, then all layers of that horizon (fibrous/amorphous) are combined together, and then split according Table D1 or equation (D1). The temperature of each new layer is determined by linear interpolation of the nearest soil temperatures of old organic soil structure. Soil freezing/thawing fronts are reassigned to new soil structure with the relative distance to the top of a horizon (moss, fibrous, amorphous) unchanged. Soil water content of each new organic soil layer is first retrieved by comparing the boundary of new and old soil layer structure. For example, if a new organic soil layer is completely located in an old organic soil layer, than the new organic soil layer is assigned a fraction of old organic soil layer's water content based on the ratio of thicknesses of both layers; if a new organic soil layer originated from two different old layers, the soil water content of new layer is assigned the sum of soil water contents retrieved from both old layers using the above method. After the determination of soil water content, the soil liquid and ice contents are retrieved with the position of freezing and thawing fronts in a layer.

[55] When fire occurs the unburned fibrous organic layer is converted to amorphous organic layer, following *Harden et al.* [2000]. A 2 cm fibrous organic layer is immediately added on top of amorphous organic layer. In this way, the fibrous organic layer can start accumulating litterfall and grow. When the thickness of live moss increases to 2 cm (see section D1 below), a new moss layer is added on top of the top fibrous organic layer.

D1. Growth of Live Moss

[56] The growth of moss is determined by a number of factors, including moss type, radiation, wind speed, and precipitation [*Bisbee et al.*, 2001]. In DOS-TEM, the biomass and NPP of moss are not simulated explicitly, as they are considered as part of overall vegetation biomass and NPP. However, the thickness of moss is explicitly considered for the purposes of soil temperature and moisture calculations. Moss thickness is simulated as an empirical function of years since last fire based on [*Yi et al.*, 2009b]:

$$d_{moss} = d_{moss,\max} \frac{y_{sf}}{y_{sf} + y_{half}} \quad \text{(D2)}$$

where d_{moss} is the thickness of moss (cm), $d_{moss,\max}$ is the maximum thickness of moss (m), y_{sf} is number of years since last fire (year), and y_{half} is number of year which was need for moss to reach half of $d_{moss,\max}$. In this study, we assigned 3.5 cm to $d_{moss,\max}$ and 5 to y_{half}= 5 based on *Yi et al.* [2009b].

D2. Change of the Thicknesses of Fibrous and Amorphous Layers

[57] The thicknesses of fibrous and amorphous layers are calculated using the simulated soil C content of each horizon and the equation:

$$C = ad^{\,b} \quad \text{(D3)}$$

where C is C content (gC/cm^2) of an organic horizon, d is organic horizon thickness (cm), and a and b are fitted coefficients for the fibrous or amorphous horizons (see *Yi et al.* [2009b] for more detail and estimates of a and b).

D3. Humification

[58] As the fibrous organic horizon grows thicker, the bottom layer of the fibrous organic horizon is transferred to the amorphous organic horizon. In this study, a threshold method is used to mimic the process of humification, i.e., when the fibrous organic horizon becomes thicker than the threshold, the component of the fibrous organic horizon above the threshold is transferred to the amorphous organic horizon. The threshold for starting humification is 16 and 33 cm for dry and wet black spruce stands, respectively. These values are the sum of mean and one standard deviation of fibrous organic horizons based on a soil horizon data set from numerous Canadian black spruce stands [*Yi et al.*, 2009b].

[59] **Acknowledgments.** This study was supported through grants provided to S. Yi as part of the Major State Basic Research Development Program of China (973 Program)(2007CB411502) and One Hundred People Plan of the Chinese Academy of Sciences. Other support to A. D. McGuire and other coauthors for this study include grants through the North American Carbon Program (NASA NNG05GD25G), the Arctic System Science Program (NSF OPP-0531047 and OPP-0327664), the Bonanza Creek Long-term Ecological Program (funded jointly by NSF grant DEB-0423442 and USDA Forest Service), and USGS Fate of Carbon in Alaska Landscapes Project. We thank Z. Fan, E. A. G. Shuur, and two anonymous reviewers for providing constructive reviews of previous versions of this paper.

References

Arora, V., and G. J. Boer (2005), Fire as an interactive component of dynamic vegetation models, *J. Geophys. Res.*, *110*, G02008, doi:10.1029/2005JG000042.

Balshi, M. S., et al. (2007), The role of historical fire disturbance in the carbon dynamics of the pan-boreal region: A process-based analysis, *J. Geophys. Res.*, *112*, G02029, doi:10.1029/2006JG000380.

Balshi, M. S., A. D. McGuire, P. Duffy, D. W. Kicklighter, and J. Melillo (2009a), Vulnerability of carbon storage in North American boreal forests to wildfires during the 21st century, *Global Change Biol.*, *15*, 1491–1510, doi:10.1111/j.1365-2486.2009.01877.x.

Balshi, M. S., A. D. McGuire, P. Duffy, M. Flannigan, J. Walsh, and J. Melillo (2009b), Assessing the response of area burned to changing climate in western boreal North America using a Multivariate Adaptive Regression Splines (MARS) approach, *Global Change Biol.*, *15*, 578–600, doi:10.1111/j.1365-2486.2008.01679.x.

Bessie, W. C., and E. A. Johnson (1995), The relative importance of fuels and weather on fire behavior in subalpine forests, *Ecology*, *76*, 747–762.

Bisbee, K. E., S. T. Gower, J. M. Norman, and E. V. Nordheim (2001), Environmental controls on ground cover species composition and productivity in a boreal black spruce forest, *Oecologia*, *129*, 261–270.

Bond-Lamberty, B., S. D. Peckham, D. E. Ahl, and S. T. Gower (2007), Fire as the dominant driver of central Canadian boreal forest carbon balance, *Nature*, *450*, 89–92.

Burn, C. R. (1998), The response (1958–1997) of permafrost and near-surface ground temperatures to forest fire, Takhini River valley, southern Yukon Territory, *Can. J. Earth Sci.*, *35*, 184–199.

Carrasco, J. J., J. C. Neff, and J. Harden (2006), Modeling physical and biogeochemical controls over carbon accumulation in a boreal forest soil, *J. Geophys. Res.*, *111*, G02004, doi:10.1029/2005JG000087.

Chen, W., J. Chen, D. Price, and J. Cihlar (2002), Effects of stand age on net primary productivity of boreal black spruce forests in Ontario, Canada, *Can. J. For. Res.*, *32*, 833–842.

Clein, J. S., A. D. McGuire, X. Zhang, D. Kicklighter, J. Melillo, S. C. Wofsy, P. G. Jarvis, and J. M. Massheder (2002), Historical and projected carbon balance of mature black spruce ecosystems across North-America: The role of carbon-nitrogen interactions, *Plant Soil*, *242*, 15–32.

Cumming, S. G. (2001), Forest type and wildfire in the Alberta boreal mixedwood: What do fires burn?, *Ecol. Appl.*, *11*, 97–110.

Davidson, E. A., and I. A. Janssens (2006), Temperature sensitivity of soil carbon decomposition and feedbacks to climate change, *Nature*, *440*, 165–173.

Dunn, A. L., C. C. Barford, S. C. Wofsy, M. L. Goulden, and B. C. Daube (2007), A long-term record of carbon exchange in a boreal black spruce forest: Means, responses to interannual variability, and decadal trends, *Global Change Biol.*, *13*, 577–590.

Euskirchen, S. E., et al. (2006), Importance of recent shifts in soil thermal dynamics on growing season length, productivity, and carbon sequestration in terrestrial high-latitude ecosystems, *Global Change Biol.*, *12*, 731–750.

Euskirchen, S. E., A. D. McGuire, and F. S. Chapin III (2007), Energy feedbacks of northern high-latitude ecosystems to the climate system due to reduced snow cover during 20th century warming, *Global Change Biol.*, *13*, 2425–2438.

Fan, Z., J. C. Neff, J. W. Harden, and K. P. Wickland (2008), Boreal soil carbon dynamics under a changing climate: A model inversion approach, *J. Geophys. Res.*, *113*, G04016, doi:10.1029/2008JG000723.

Flannigan, M., K. A. Logan, B. D. Amiro, W. R. Skinner, and B. J. Stocks (2005), Future area burned in Canada, *Clim. Change*, *77*, 1–16.

French, N. H. F., E. S. Kasischke, and D. G. Williams (2002), Variability in the emission of carbon-based trace gases from wildfire in the Alaskan boreal forest, *J. Geophys. Res.*, *107*, 8151, doi:10.1029/2001JD000480 [printed *108*(D1), 2003].

Frolking, S., N. T. Roulet, T. R. Moore, P. J. Richard, M. Lavoie, and S. D. Muller (2001), Modeling northern peatland decomposition and peat accumulation, *Ecosystems*, *4*, 479–498.

Funk, D. W., E. R. Pullman, K. M. Peterson, C. M. Patrick, and W. D. Billings (1994), Influence of water table on carbon dioxide, carbon monoxide, and methane fluxes from taiga bog microcosms, *Global Biogeochem. Cycles*, *8*, 271–278.

Gillett, N. P., A. J. Weaver, F. W. Zwiers, and M. D. Flannigan (2004), Detecting the effect of climate change on Canadian forest fires, *Geophys. Res. Lett.*, *31*, L18211, doi:10.1029/2004GL020876.

Goulden, M. L., A. M. S. McMillan, G. C. Winston, A. V. Rocha, K. L. Manies, J. W. Harden, and B. P. Bond-Lamberty (2010), Patterns of NPP, GPP, respiration, and NEP during boreal forest succession, *Global Change Biol.*, doi:10.1111/j.1365-2486.2010.02274.x, in press.

Gower, S. T., R. E. McMurtrie, and D. Murty (1996), Aboveground net primary production decline with stand age: Potential causes, *Trends Ecol. Evol.*, *11*, 378–382.

Gower, S. T., J. G. Vogel, J. M. Norman, C. J. Kucharik, P. L. Steele, and T. K. Stow (1997), Carbon distribution and aboveground net primary production in aspen, jack pine, and black spruce stands in Saskatchewan and Manitoba, Canada, *J. Geophys. Res.*, *102*(D24), 29,029–29,041.

Grant, R. F. (2004), Modeling topographic effects on net ecosystem productivity of boreal black spruce forests, *Tree Physiol.*, *24*, 1–18.

Harden, J., S. E. Trumbore, B. J. Stocks, A. I. Hirsch, S. T. Gower, K. P. O. Neill, and E. Kasischke (2000), The role of fire in the boreal carbon budget, *Global Change Biol.*, *6*, suppl. 1, 174–184.

Harden, J. W., R. Meier, C. Darnel, D. K. Swanson, and A. D. McGuire (2003), Soil drainage and its potential for influencing wildfire in Alaska, in *Studies in Alaska by the U.S. Geological Survey*, edited by J. Galloway, *U.S. Geol. Surv. Prof. Pap.*, *1678*.

Harden, J., J. C. Neff, D. V. Sandberg, M. R. Turetsky, R. D. Ottmar, G. Gleixner, T. Fries, and K. L. Manies (2004), Chemistry of burning the forest floor during the FROSTFIRE experimental burn, interior Alaska, 1999, *Global Biogeochem. Cycles*, *18*, GB3014, doi:10.1029/2003GB002194.

Harden, J. W., K. L. Manies, J. C. Neff, and M. R. Turetsky (2006), Effects of wildfire and permafrost on soil organic matter and soil climate in interior Alaska, *Global Change Biol.*, *12*, 1–13, doi:10.1111/j.1365-2486.2006.01255.x.

Hayes, D. J., A. D. McGuire, D. W. Kicklighter, T. J. Burnside, and J. M. Melillo (2010), The effects of land cover and land use change on the contemporary carbon balance of the arctic and boreal ecosystems of northern Eurasia, in *Arctic Land Cover and Land Use in a Changing Climate*, edited by G. Gutman, chap. 5, Springer, New York, in press.

Jobbagy, E. G., and R. B. Jackson (2000), The vertical distribution of soil organic carbon and its relation to climate and vegetation, *Ecol. Appl.*, *10*, 423–436.

Johnstone, J. F. (2006), Response of boreal plant communities to variations in previous fire-free interval, *Int. J. Wildland Fire*, *15*, 497–508.

Johnstone, J. F., and S. F. Chapin (2006), Effects of soil burn severity on post-fire tree recruitment in boreal forest, *Ecosystems*, *9*, 14–31.

Johnstone, J. F., and E. Kasischke (2005), Stand-level effects of soil burn severity on postfire regeneration in a recently burned black spruce forest, *Can. J. For. Res.*, *35*, 2151–2163.

Kanamitsu, M., et al. (2002), NCEP-DOE AMIP-II Reanalysis (R-2), *Bull. Am. Meteorol. Soc.*, *83*, 1631–1643.

Kane, E. S., E. S. Kasischke, D. W. Valentine, M. R. Turetsky, and A. D. McGuire (2007), Topographic influences on wildfire consumption of soil organic carbon in interior Alaska: Implications for black carbon accumulation, *J. Geophys. Res.*, *112*, G03017, doi:10.1029/2007JG000458.

Karunaratne, K. C., and C. R. Burn (2004), Relations between air and surface temperature in discontinuous permafrost terrain near Nayo, Yukon Territory, *Can. J. Earth Sci.*, *41*, 1437–1451.

Kasischke, E. S., and J. F. Johnstone (2005), Variation in postfire organic layer thickness in a black spruce forest complex in interior Alaska and its effects on soil temperature and moisture, *Can. J. For. Res.*, *35*, 2164–2177.

Kasischke, E. S., and M. R. Turetsky (2006), Recent changes in the fire regime across the North American boreal region—Spatial and temporal patterns of burning across Canada and Alaska, *Geophys. Res. Lett.*, *33*, L09703, doi:10.1029/2006GL025677.

Kasischke, E. S., E. J. Hyer, P. C. Novelli, L. P. Bruhwiler, N. H. F. French, A. I. Sukhinin, B. Hewitson, and B. J. Stocks (2005), Influences of boreal fire emissions on northern hemisphere atmospheric carbon and carbon monoxide, *Global Biogeochem. Cycles*, *19*, GB1012, doi:10.1029/2004GB002300.

Kasischke, E. S., T. S. Rupp, and D. L. Verbyla (2006), Fire trends in the Alaskan boreal forest, in *Alaska's Changing Boreal Forest*, edited by F. S. Chapin III et al., pp. 285–301, Oxford Univ. Press, New York.

Kasischke, E. S., et al. (2010), Alaska's changing fire regime—Implications for the vulnerability of its boreal forests, *Can. J. For. Res.*, *40*(7), 1313–1324.

Keeling, C. D., and T. P. Whorf (2005), Atmospheric CO_2 records from sites in the SIO air sampling network, in *Trends: A Compendium of Data on Global Change*, Carbon Dioxide Inf. and Anal. Cent., Oak Ridge Natl. Lab., U.S. Dep. of Energy, Oak Ridge, Tenn.

Klene, A. E., F. E. Nelson, and N. I. Shiklomanov (2001), The n-factor as a tool in geocryological mapping: Seasonal thaw in the Kuparuk River basin, Alaska, *Phys. Geogr.*, *22*, 449–466.

Lawrence, D. M., and A. G. Slater (2008), Incorporating organic soil into a global climate model, *Clim. Dyn.*, doi:10.1007/s00382-007-0278-1.

Liljedahl, A., L. D. Hinzman, R. Busey, and K. Yoshikawa (2007), Physical short-term changes after a tussock tundra fire, Seward Peninsula, Alaska, *J. Geophys. Res.*, *112*, F02S07, doi:10.1029/2006JF000554.
Liu, H., and J. T. Randerson (2008), Interannual variability of surface energy exchange depends on stand age in a boreal forest fire chronosequence, *J. Geophys. Res.*, *113*, G01006, doi:10.1029/2007JG000483.
Liu, H., J. T. Randerson, J. Lindfors, and F. S. Chapin III (2005), Changes in the surface energy budget after fire in boreal ecosystems of interior Alaska: An annual perspective, *J. Geophys. Res.*, *110*, D13101, doi:10.1029/2004JD005158.
Mack, M., K. K. Treseder, K. L. Manies, J. Harden, A. G. Schuur, J. G. Vogel, J. T. Randerson, and S. F. Chapin (2008), Recovery of aboveground plant biomass and productivity after fire in mesic and dry black spruce forests of interior Alaska, *Ecosystems*, doi:10.1007/s10021-007-9117-9.
MacKay, J. R. (1995), Active layer changes (1968 to 1993) following the forest-tundra fire near Inuvik, N.W.T., Canada, *Arct. Alp. Res.*, *27*, 323–336.
Manies, K. L., J. Harden, B. Bond-Lamberty, and K. P. O'Neill (2005), Woody debris along an upland chronosequence in boreal Manitoba and its impact on long-term carbon storage, *Can. J. For. Res.*, *35*, 472–482.
Manies, K. L., J. W. Harden, and H. Veldhuis (2006), Soil data from a moderately well and somewhat poorly drained fire chronosequence near Thompson, Manitoba, Canada, *U.S. Geol. Surv. Open File Rep., 2006-1291*, 17 pp.
McGuire, A. D., J. Melillo, E. G. Jobbagy, D. Kicklighter, A. L. Grace, B. Moore, and C. J. Vorosmarty (1992), Interactions between carbon and nitrogen dynamics in estimating net primary productivity for potential vegetation in North America, *Global Biogeochem. Cycles*, *6*, 101–124.
McGuire, A. D., L. G. Anderson, T. R. Christensen, S. Dallimore, L. Guo, D. J. Hayes, M. Heimann, T. D. Lorenson, R. W. Macdonald, and N. Roulet (2009), Sensitivity of the carbon cycle in the Arctic to climate change, *Ecol. Monogr.*, *79*, 523–555.
Melillo, J. M., A. D. McGuire, D. W. Kicklighter, B. Moore III, C. J. Vorosmarty, and A. L. Schloss (1993), Global climate change and terrestrial net primary production, *Nature*, *63*, 234–240.
Mitchell, T. D., and P. D. Jones (2005), An improved method of constructing a database of monthly climate observations and associated high-resolution grids, *Int. J. Climatol.*, *25*, 693–712.
O'Connell, K. B., S. T. Gower, and J. M. Norman (2003), Net ecosystem production of two contrasting boreal black spruce forest communities, *Ecosystems*, *6*, 248–260.
O'Neill, K. P., E. Kasischke, and D. D. Richter (2002), Environmental controls on soil CO_2 flux following fire in black spruce, white spruce, and aspen stands of interior Alaska, *Can. J. For. Res.*, *32*, 1525–1541.
Parton, W. J., D. Schimel, V. C. Cole, and D. Ojima (1987), Analysis of factors controlling soil organic levels of grasslands in the Great Plains, *Soil Sci. Soc. Am. J.*, *51*, 1173–1179.
Prescott, C. E., D. G. Maynard, and R. Laiho (2000), Humus in northern forests: Friend or foe?, *For. Ecol. Manage.*, *133*, 23–36.
Raich, J. W., E. B. Rastetter, J. Melillo, D. Kicklighter, P. A. Steudler, B. J. Peterson, A. L. Grace, B. Moore, and C. J. Vorosmarty (1991), Potential net primary productivity in South America: Application of a global model, *Ecol. Appl.*, *1*, 399–429.
Rastetter, E. B., A. W. King, B. J. Cosby, G. M. Hornberger, R. V. O'Neill, and J. E. Hobbie (1992), Aggregating fine-scale ecological knowledge to model coarser-scale attributes of ecosystems, *Ecol. Appl.*, *2*, 55–70.
Renkin, R. A., and D. G. Despain (1992), Fuel moisture, forest type, and lightning-caused fire in Yellowstone National Park, *Can. J. For. Res.*, *22*, 37–45.
Ruess, R. W., R. L. Hendrick, A. J. Burton, K. S. Pregitzer, B. Sveinbjornsson, M. F. Allen, and G. E. Maurer (2003), Coupling fine root dynamics with ecosystem carbon cycling in black spruce forests of Interior Alaska, *Ecol. Monogr.*, *73*, 643–662.
Schuur, E. A. G., et al. (2008), Vulnerability of permafrost carbon to climate change: Implications for the global carbon cycle, *BioScience*, *58*, 701–714.
Simard, M., N. Lecomte, Y. Bergeron, P. Y. Bernier, and D. Pare (2007), Forest productivity decline caused by successional paludification of boreal soils, *Ecol. Appl.*, *17*, 1619–1673.
Steele, S. J., S. T. Gower, J. G. Vogel, and J. M. Norman (1997), Root mass, net primary production and turnover in aspen, jack pine and black spruce forests in Saskatchewan and Manitoba, Canada, *Tree Physiol.*, *17*, 577–587.
Tarnocai, C., J. G. Canadell, G. Mazhitova, E. A. G. Schuur, P. Kuhry, and S. Zimov (2009), Soil organic carbon pools in the northern circumpolar permafrost region, *Global Biogeochem. Cycles*, *23*, GB2023, doi:10.1029/2008GB003327.
Thonicke, K., S. Venevsky, S. Sitch, and W. Cramer (2001), The role of fire disturbance for global vegetation dynamics: Coupling fire into a Dynamic Global Vegetation Model, *Glob. Ecol. Biogeogr.*, *10*, 661–677.
Tian, H., J. M. Melillo, D. W. Kicklighter, A. D. McGuire, and J. Helfrich (1999), The sensitivity of terrestrial carbon storage to historical climate variability and atmospheric CO_2 in the United States, *Tellus, Ser. B*, *51*, 414–452.
Van Cleve, K., C. T. Dyrness, L. A. Viereck, J. Fox, F. S. Chapin III, and W. Oechel (1983), Taiga ecosystem in interior Alaska, *BioScience*, *33*, 39–44.
Viereck, L. A., and W. F. Johnston (1990), Black spruce, in *Silvics of North America*, vol. 1, *Conifers*, edited by R. M. Burns and B. H. Honkala, pp. 227–237, For. Serv., U.S. Dep. of Agric., Washington, D. C.
Vogel, J. G., B. Bond-Lamberty, A. G. Schuur, S. T. Gower, M. Mack, K. B. O. Connell, D. W. Valentine, and R. W. Ruess (2008), Carbon allocation in boreal black spruce forests across regions varying in soil temperature and precipitation, *Global Change Biol.*, *14*, 1503–1516.
Yi, S., A. M. Arain, and M.-K. Woo (2006), Modifications of a land surface scheme for improved simulation of ground freeze-thaw in northern environments, *Geophys. Res. Lett.*, *33*, L13501, doi:10.1029/2006GL026340.
Yi, S., et al. (2009a), Interactions between soil thermal and hydrological dynamics in the response of Alaska ecosystems to fire disturbance, *J. Geophys. Res.*, *114*, G02015, doi:10.1029/2008JG000841.
Yi, S., K. Manies, J. Harden, and A. D. McGuire (2009b), Characteristics of organic soil in black spruce forests: Implications for the application of land surface and ecosystem models in cold regions, *Geophys. Res. Lett.*, *36*, L05501, doi:10.1029/2008GL037014.
Zhang, Y., W. Chen, and J. Cihlar (2003), A process-based model for quantifying the impact of climate change on permafrost thermal regimes, *J. Geophys. Res.*, *108*(D22), 4695, doi:10.1029/2002JD003354.
Zhuang, Q., V. E. Romanovsky, and A. D. McGuire (2001), Incorporation of a permafrost model into a large-scale ecosystem model: Evaluation of temporal and spatial scaling issues in simulating soil thermal dynamics, *J. Geophys. Res.*, *106*, 33,649–33,670.
Zhuang, Q., A. D. McGuire, K. P. O'Neill, J. W. Harden, V. E. Romanovsky, and J. Yarie (2002), Modeling soil thermal and carbon dynamics of a fire chronosequence in interior Alaska, *J. Geophys. Res.*, *107*, 8147, doi:10.1029/2001JD001244 [printed *108*(D1), 2003].
Zhuang, Q., et al. (2003), Carbon cycling in extratropical terrestrial ecosystems of the Northern Hemisphere during the 20th century: A modeling analysis of the influences of soil thermal dynamics, *Tellus, Ser. B*, *55*, 751–776.
Zimov, S. A., S. P. Davidov, G. M. Zimova, A. I. Davidova, F. S. Chapin, M. C. Chapin, and J. F. Reynolds (1999), Contribution of disturbance to increasing seasonal amplitude of atmospheric CO_2, *Science*, *284*, 1973–1976.

J. Harden and K. Manies, U.S. Geological Survey, Menlo Park, CA 94025, USA.

E. Kasischke, Department of Geography, University of Maryland, 2181 LeFrak Hall, College Park, MD 20742, USA.

M. Mack, Department of Botany, University of Florida, Gainesville, FL 32611, USA.

A. D. McGuire, Alaska Cooperative Fish and Wildlife Research Unit, U.S. Geological Survey, University of Alaska Fairbanks, Fairbanks, AK 99775, USA.

M. Turetsky, Department of Integrative Biology, University of Guelph, Guelph, ON N1G 2W1, Canada.

S. Yi, State Key Laboratory of Cryosphere Sciences, Cold and Arid Regions Environmental and Engineering Research Institute, Lanzhou, Gansu 730000, China. (yis@lzb.ac.cn)